The Meteoritical Society

Meteoritics & Planetary Science 1–9 (2022)
doi: 10.1111/maps.13785

Ultrafast structural response of shock-compressed plagioclase

Arianna E. GLEASON[1]*, Sulgiye PARK[2], Dylan R. RITTMAN[2], Alessandra RAVASIO[3], Falko LANGENHORST[4,5], Riccardo M. BOLIS[3], Eduardo GRANADOS[1], Sovanndara HOK[2], Thomas KROLL[1], Marcin SIKORSKI[6], Tsu-Chien WENG[7], Hae Ja LEE[2], Bob NAGLER[2], Thomas SISSON[8], Zhou XING[1], Diling ZHU[1], Gabriele GIULI[9], Wendy L. MAO[2], Siegfried H. GLENZER[1], Dimosthenis SOKARAS[1], and Roberto ALONSO-MORI[1]*

[1]SLAC National Accelerator Laboratory, Menlo Park, California 94025, USA
[2]Department of Geological Sciences, Stanford University, Stanford, California 94305, USA
[3]LULI - CNRS, Ecole Polytechnique, Palaiseau, France
[4]Institute of Geoscience, Friedrich Schiller University Jena, Carl-Zeiss-Promenade 10, Jena 07745, Germany
[5]School of Ocean and Earth Science and Technology, Hawai'i Institute of Geophysics and Planetology, University of Hawai'i at Manoa, Honolulu, Hawai'i 96822, USA
[6]European XFEL GmbH, Schenefeld, Germany
[7]School of Physical Science and Technology, Shanghai Tech University, Shanghai 201210, China
[8]United States Geological Survey, Menlo Park, California 94025, USA
[9]School of Science and Technology, Geology Division, University of Camerino, Camerino I-62032, Italy
*Corresponding authors. E-mails: ariannag@stanford.edu; robertoa@slac.stanford.edu

(Received 11 February 2021; revision accepted 28 December 2021)

Abstract–Meteor impacts can induce unique pressure-dependent structural changes in minerals due to the propagation of shock waves. Plagioclase—ubiquitous throughout the Earth's crust, extraterrestrial bodies, and meteorites—is commonly used for reconstructing the impact history and conditions of the parent bodies. However, there have been unresolved inconsistencies in the interpretation of shock transformations across previous studies: The pressure at which amorphization begins and the process by which it occurs is the subject of ongoing debate. Here, we utilize time-resolved in situ X-ray diffraction (XRD) to probe the phase transformation pathway of plagioclase during shock compression at a sub-nanosecond timescale. Direct amorphization begins at pressures much lower than what was previously assumed, just above the Hugoniot elastic limit of 5 GPa, with full amorphization to a high-density amorphous phase, observed at 32(10) GPa and 20 ns. Upon release, the material partially recrystallizes back into the original structure, demonstrating a memory effect.

INTRODUCTION

Plagioclase feldspars, framework silicates forming a solid solution of albite ($NaAlSi_3O_8$, Ab) and anorthite ($CaAl_2Si_2O_8$, An), are the most abundant group of minerals found in the Earth's crust. Their unique behavior under shock compression and prevalence on the Earth and the surfaces of other extraterrestrial bodies—such as Mars, the Moon, and asteroids—makes them a widely used indicator for diagnosing impact events in the terrestrial bodies (Becker et al., 2004; French & Koeberl, 2010; Ostertag, 1983; Sharp & DeCarli, 2006; Stöffler et al., 1991). The shock waves generated by these impacts cause plagioclase to undergo a variety of shock-induced structural transformations and processes such as fracturing, planar deformation feature (PDF) formation, amorphization (i.e., maskelynite formation), high-pressure polymorphism (e.g., hollandite-structured polymorphs; Tschauner, 2019), and melting

Arianna E. Gleason, Sulgiye Park, and Dylan R. Rittman contributed equally.

(Gibbons & Ahrens, 1977; Jaret et al., 2015; Ostertag, 1983; Sims et al., 2019; Stöffler et al., 1991). These modifications, particularly PDFs and maskelynite, that form over a narrow pressure interval, are often used as geologic indicators of peak shock pressure (Fritz et al., 2005; Stöffler, 1974; Stöffler et al., 1991). PDFs are often observed parallel to the (001), (010), (100), (120), (130) planes and/or can occur as isotropic bands parallel to twin lamellae (Pittarello et al., 2020). Ostertag (1983) also found evidence for narrow parallel sets of PDFs in experimentally shocked plagioclases. The amorphous nature of these thinner lamellae was subsequently shown by numerous transmission electron miscroscopy (TEM) observations in terrestrial impact rocks and heavily shocked chondrites (e.g., Langenhorst et al., 1995). This transition of plagioclase to maskelynite (i.e., diaplectic glass with feldspar composition) occurs continuously by an increase in amorphous phase volume as a function of increasing pressure (Stöffler et al., 1991).

Due to the importance of feldspar in geological and planetary sciences, there is a rich literature detailing structural changes under shock compression—though its use as a shock barometer remains purely empirical. This is in part due to the open crystal structures and resulting high compressibilities of framework silicates enabling different sequences or combinations of structural modifications (e.g., bending and buckling of Si, O tetrahedra or octahedra, and changes in long- and short-range ordering). For example, the Hugoniot elastic limit (HEL) of the feldspar, above which irreversible atomic motion (i.e., plastic flow) occurs, is ~5 GPa (Ahrens et al., 1969). However, the first optical microscopy evidence of plastic flow in shocked recovered plagioclase does not occur until ~15 GPa (e.g., Sharp & DeCarli, 2006; Stöffler, 1974). Interestingly, quartz PDF calibration for shock barometry is well documented and robust based on experiments; however, due to the likely influence of composition, complex crystal chemistry, and apparent post-shock annealing, a rigorous calibration of feldspar PDFs is still unresolved.

Observations of changes in shock and particle velocities, recorded during shock compression, suggested a material transformation into a two-phase regime—though a direct measure differentiating these two proposed phases was not available. Ahrens et al. (1969) used velocimetry to suggest the transformation of plagioclase to a high-pressure polymorph—proposed to possess the hollandite-type crystal structure that reverts to an amorphous phase upon release. This crystalline phase is thought to be fully formed by ~40 GPa and preceded by a large mixed-phase regime (Ahrens et al., 1969). The Hugoniot curve (Fig. S1 in supporting information) shows a discrete increase in compressibility between the ~5 GPa HEL and the ~40 GPa high-pressure phase regime, with the start of the mixed-phase regime being set at 15 GPa, as defined by previously published optical data (Ahrens et al., 1969; Langenhorst, 1989; Ostertag, 1983). More recent studies have clearly identified the formation of maskelynite from shocked plagioclase via solid-state transformation. The structure factor and pair distribution functions of the maskelynite grains and fused glass were studied by Jaret et al. (2015), finding a higher degree of atomic ordering in maskelynite, compared with fused glass, which exhibited continuous random networks. The higher degree of ordering in diaplectic glass compared with fused glass agrees with Diemann and Arndt (1984).

The recent development of probes capable of interrogating structural changes in situ during shock processes has made direct measurements of the phase transitions possible. Here, we take advantage of X-ray-free electron laser (XFEL)-based time-resolved in situ X-ray diffraction (XRD) to present the first structural study of plagioclase during shock compression—providing evidence of direct amorphization. In addition, these results uniquely reveal that previously considered distinct shock stages are in fact derived from a single continuous mechanism.

RESULTS

Polycrystalline samples of plagioclase (specifically the mineral labradorite with a composition of An52.5Ab47.5) were shock compressed at the matter in extreme conditions (MEC) end station of the linac coherent light source (LCLS) using 8 keV (λ = 1.5498 Å) X-rays (Fig. 1) (Emma et al., 2010). The temporal pulse width of the X-rays is 50 fs, providing high fidelity time-resolved XRD to determine the in situ atomic structure of the material and track transformation kinetics. The X-rays probed the entirety of the sample thickness, such that XRD measured varying fractions of ambient and compressed plagioclase as a function of time delay.

Velocimetry measurements were also collected to determine the sample pressure from particle velocity using a velocity interferometer system for any reflector (VISAR) diagnostic to record free surface measurements or through a transparent quartz or LiF window (Barker & Hollenbach, 1972). For each shot, the pressure was determined using a combination of XRD to measure crystalline lattice parameters for unit cell volumes and/or velocimetry using known static and dynamic compression equations of state (Ahrens et al., 1969; Benusa et al., 2005; Dennen, 1965) (Discussion S1 and Table S1 in supporting information). The average pressure from these different methods is reported and

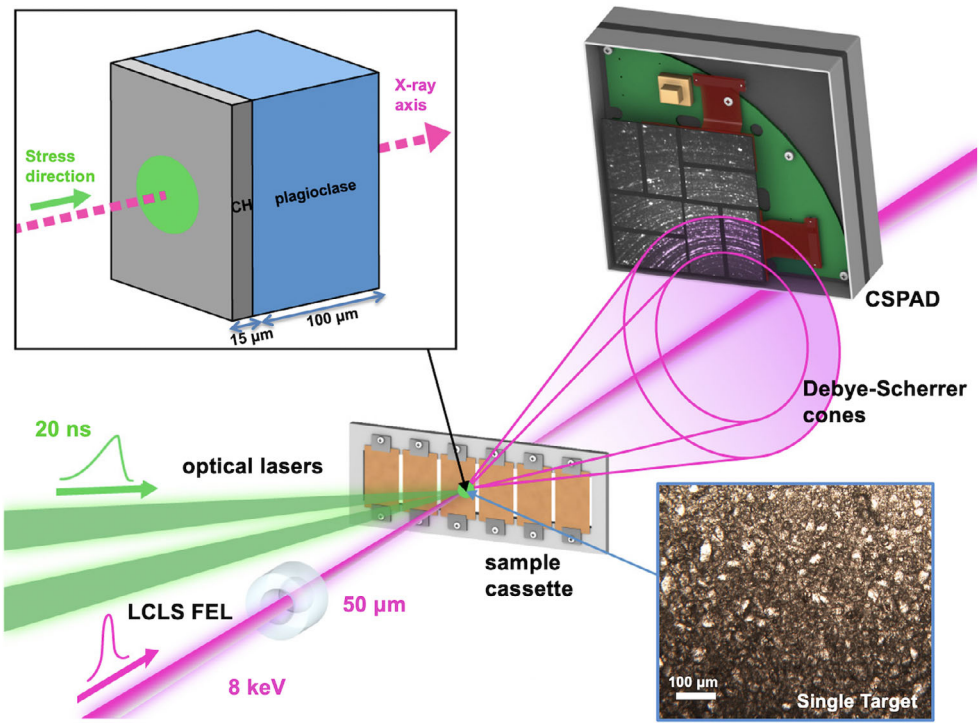

Fig. 1. Experimental configuration of optical laser drive and XFEL probe. Structural response of the sample to the high pressure–temperature conditions induced by the shock wave was probed by time-resolved XRD. Top left: a schematic of the sample geometry. Bottom right: a polarized optical micrograph of the ambient conditions preshock plagioclase sample showing its polycrystalline structure. Transmission XRD is collected during laser-driven shock compression. The optical laser (shown as 2 arm green beams) is incident on the sample forming an ablation plasma to launch a shock. XRD time slices are collected from the LCLS probe with 8 keV X-rays and a section of the Debye-Scherer cones intersected by downstream detectors at a distance of 10.5 cm (labeled CSPAD) with an angular coverage of 20–70° 2θ.

pressure uncertainty derived from the standard deviation across all values.

The In Situ Structural Response of Plagioclase to Shock Compression

In situ time-resolved XRD enables investigation of atomic-level information to determine the pressure-dependent structural evolution of a material. Representative XRD patterns of plagioclase at full compression (achieved at ~17–20 ns depending on the shock velocity), when the entire sample is at a uniform high pressure–temperature state, are shown in Fig. 2. The sample remains crystalline under compression up to 3(1) GPa. The slight increase in full width at half maximum (FWHM) at this pressure can be attributed to the microstrain induced by the uniaxial compression, as there is no significant contribution of diffuse scattering observed. At 8 ± 2 GPa, crystalline peaks are still present, but a diffuse feature has started to develop. The diffuse scattering fraction continues to increase with pressure until the entire pattern shows only a diffuse signal at 32 ± 10 GPa, in which no notable crystalline peaks are observed (Fig. S2 in supporting information).

We interpret the increase in peak FWHM and formation of diffuse features in the XRD as amorphization of plagioclase. This onset of amorphization coincides with the start of the mixed-phase regime just above the ~5 GPa HEL (Ahrens et al., 1969), continuing until the plagioclase is completely amorphized at 32 ± 10 GPa. The wide pressure range where amorphous and crystalline structures coexist is consistent with previous velocimetry measurements of shocked plagioclase (Ahrens et al., 1969). We also consider nanocrystalline formation, loss of periodicity, or stress gradients as possible causes of peak broadening.

Due to the limited Q-range of this experiment, a quantitative assessment of the structure factor and corresponding coordination changes cannot be completed. However, there is a notable trend in the change of the diffuse feature peak position and intensity as a function of shock compression. The amorphous state exhibits two broad diffuse features, centered around the *d*-spacing ~2.6 Å (first) and ~2.0 Å (second). As pressure increases, the intensity of the second diffuse scattering

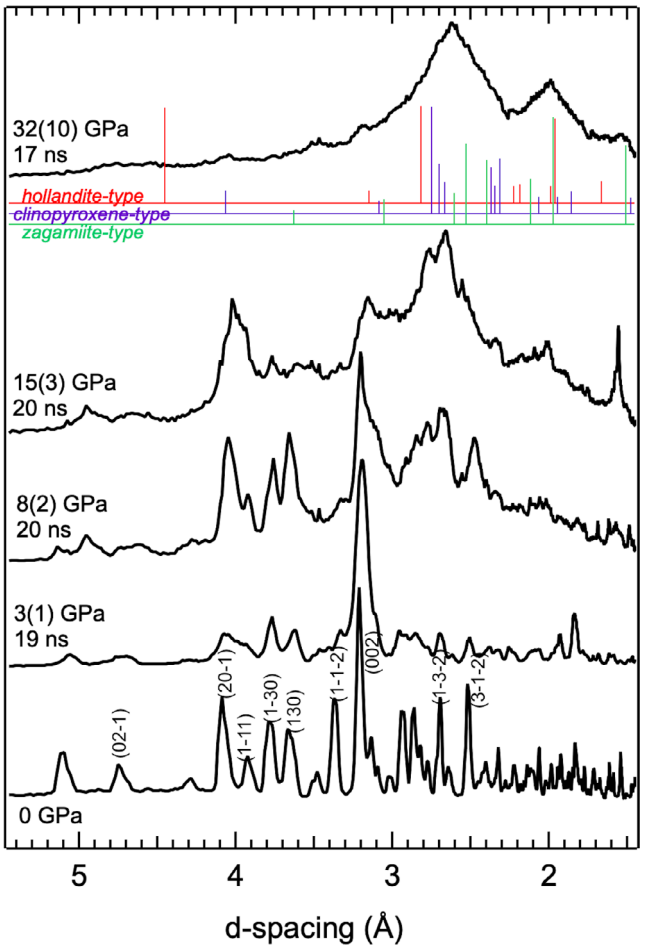

Fig. 2. Pressure-dependent structural behavior of shocked plagioclase. XRD of shocked plagioclase at approximately full compression. An amorphous phase is produced above the ~5 GPa HEL with its phase fraction increasing with pressure. A qualitative comparison of calculated model phases, such as a hollandite-type (Ferroir et al., 2006) in red, a clinopyroxene-type (Posner et al., 2014) in purple, and a zagamiite-type (Gautron et al. [1999] with an EoS from Caracas & Boffa Ballaran [2010]) in green is provided for the highest pressure trace, suggesting a zagamiite-type or hollandite-type topology forms.

increases relative to the first (Fig. S2). This trend in relative peak intensity change is evidence of a pressure-induced loss of medium-range order and increase in cation coordination number, wherein the sixfold coordination of silicon and aluminum increases as a function of increasing pressure (Gleason et al., 2017; Itie et al., 1989; Meade et al., 1992; Tschauner et al., 2006). During shock release, diffuse scattering shifts to larger *d*-spacing, which is attributed to glass structural relaxation—a first-order transition, in which the short-range order of glass continuously evolves as pressure releases.

Several studies note the formation of high-pressure phases in shock-compressed feldspar (Ahrens et al., 1969), such as the hollandite-structured high-pressure phase with a mixed plagioclase composition $(Na_x, Ca_{1-x})Al_{2+x}Si_{3-x}O_8$ (Ahrens et al., 1969) which is called lingunite (Liu & El Goresey, 2007). In fact there are a number of studies which identify and elaborate on the structural and compositional differences between hollandite-type polymorphs, such as lingunite (Agarwal et al., 2016; Gillet et al., 2000; Langenhorst & Dressler, 2003), liebermannite (Ma et al., 2018), and stöfflerite (Tschauner et al., 2021), where An >50 is stöfflerite and Ab>50 is lingunite. However, none of these crystalline minerals were observed in our experiments during either the compression or release stages. Instead, in situ data on the high-pressure phase indicate a complete amorphization at the highest measured pressure of ~32(10) GPa. Occurrence of an amorphous phase as opposed to a crystalline phase at high pressure is reasonable for plagioclase under shock compression. The formation of any of these high-pressure polymorphs, for example, lingunite or stöfflerite, would be reconstructive, requiring the breaking of bonds and diffusion of atoms into new positions. Furthermore, the many cation species in plagioclase necessitates many distinct cation sites in a crystalline structure. These requirements make atomic ordering difficult, especially on short timescales of shock compression where atomic motion to thermodynamically preferred positions is kinetically inhibited, resulting in a metastable amorphous phase.

The direct production of an amorphous phase at high pressure has important implications for the formation of maskelynite: The tendency for plagioclase to readily amorphize for all pressures greater than the HEL supports the premise that the disordered maskelynite can be produced without melting. Melting can also occur upon quasi-isentropic release, which creates a zero-pressure, high-temperature state (Fig. S3 in supporting information). However, entropy-density data (Ahrens & O'Keefe, 1972), cross-referenced with density-pressure data (Ahrens et al., 1969), show that compression to ~50 GPa is necessary to produce melt upon release. Thus, we present the first in situ measurement of amorphization of plagioclase during shock compression. Our data corroborate Jaret et al.'s (2015) findings on maskelynite, also observing a notable degree of disordering at long length scales upon compression. This disordering in our diaplectic maskelynite glass partially recovers during pressure release—the phenomenon related to the memory effect, which would have been absent in the case of fused plagioclase glass with an increased degree of disordering.

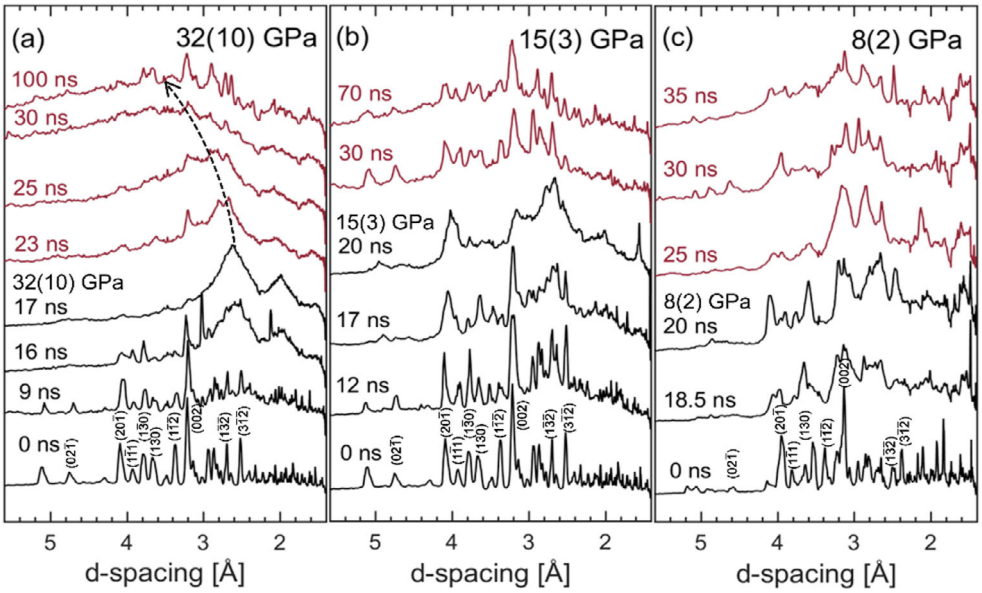

Fig. 3. Time-resolved structural behavior of plagioclase under shock compression and decompression. a–c) Raw XRD patterns of shocked plagioclase, without background subtraction, at a variety of time delays (on compression—black traces; on release—red traces).

Time-Resolved Structural Evolution Under Shock Compression and the Memory Effect

The time-dependent structural evolution of plagioclase offers critical information on the kinetics of the transformation and metastability of the high-pressure amorphous phase. Representative time-resolved XRD patterns of plagioclase shocked to 8(2), 15(3), and 32 (10) GPa are shown in Fig. 3. Notably, the behavior is similar for all shock pressures above the HEL, indicating a unified mechanism underlying the shock response of plagioclase. Amorphous fraction, denoted by an intensification of diffuse scattering, increases as the shock wave propagates through the sample with full compression occurring at $\approx\leq$20 ns at 32(10) GPa (Fig. 3d). After 20 ns, the duration of the drive laser pulse is complete and the material begins to release to an ambient-pressure, high-temperature state. As expected, the decrease in pressure during release drives the center of the first amorphous diffuse feature at *d*-spacing ~2.6 Å to shift to larger *d*-spacing (indicated by an arrow in Fig. 3a). As in the case of Fig. 2, the transition of higher density amorphous (HDA) phase with increased cation coordination to lower density amorphous (LDA) phase at longer time delay suggests glass structure relaxation, and further explains the greater extrapolated zero-pressure density of the high-pressure phase relative to the recovered glass.

LDA glass formation is followed by recrystallization back into the original structure at extended time delays. The recovery of the plagioclase structure upon quenching is consistent with static diamond anvil cell results, which report on the pressure-induced memory effects (Ostertag, 1983; Sims et al., 2020; Stöffler, 1974). Studies show that decompression rate does not influence reversion, but there is a critical pressure and durability at high pressure, below which recovery into initial structure can take place (Sims et al., 2020; Stöffler et al., 1991). Sims et al. (2020) indicate that given enough pressure and time, energy and kinetics enable atoms to rearrange themselves in a manner that attains aperiodicity upon decompression. In agreement with literature, our study shows a trend of recovery for labradorite upon release (Sims et al., 2020; Stöffler et al., 1991). The nature of dynamic compression lends itself to a higher critical pressure of 32(10) GPa due to the differing strain rate, but the nature of recoverability remains the same. During release around ~23 ns, minor traces of diffuse scattering fraction are observed in both integrated and two-dimensional diffraction images (Fig. S3). At 100 ns, almost full recovery is observed. The intensity of crystalline peaks is diminished, but the *d*-spacing of each observable crystalline peak is in complete correspondence with an unshocked pattern.

The recovery of crystallinity appears sooner for plagioclase shocked to pressures below its critical point. Samples shocked to 8(2) and 15(3) GPa do not exhibit full amorphization, and almost all crystallinity reappears at ~25–30 ns; ~5–10 ns after the materials had reached its peak pressure. The earlier onset of recrystallization for materials shocked to 8(2) and 15(3) GPa is anticipated

given that the remnants of long-range periodicity should enable a lower energetic barrier to reform the primitive structure. Our observation of the recovery of the plagioclase structure upon release demonstrates, for the first time, that a memory effect exists even at the very short timescale of laser shock compression. The amorphous fraction seems to inherit and conserve structural elements of plagioclase, enabling it to reconvert partially to the crystalline state upon decompression.

DISCUSSION

Seemingly incongruent results between ex situ optical and in situ XRD data in the formation of atomistic-scale disordering may only be an apparent discrepancy due to timescale. Velocimetry and in situ XRD are done at high pressure during dynamic compression to show the transient state—and not the final state. The optical observations are done ex situ after the recovery of the structure by the memory effect. Notably, we observe partial-to-complete amorphization of plagioclase at full compression for all pressures above the HEL of ~5 GPa, which is consistent with velocimetry measurements that observed a large mixed-phase regime starting at ~5 GPa (Stöffler et al., 1991). An apparent inconsistency with optical studies that only report amorphous material in excess of ~15 GPa (Cygan et al., 1989; Langenhorst, 1994) is likely due to the memory effect. Here, amorphization on compression is recovered to a crystalline state on decompression such that ex situ investigations would not detect any amorphous material. Transmission electron microscopy resolved PDFs in α-quartz as thin as 30 nm that increased in size and population as a function of pressure (Gibbons & Ahrens, 1977; Ostertag, 1983; Stöffler, 1967, 1974).

Formation Mechanism of Maskelynite

The entirety of a plagioclase grain becomes amorphous as PDFs coarsen and increase in number, marking the onset of maskelynite formation (Stöffler et al., 1991). Thus, maskelynite may not be atomistically distinct from amorphous PDFs. Rather, the differentiation is based on microstructure. This is consistent with the gradual increase in amorphous phase fraction as a function of pressure observed here. Furthermore, the previously defined ~45 GPa threshold for maskelynite formation (Gibbons & Ahrens, 1977; Ostertag, 1983; Stöffler, 1967, 1974) is consistent with the complete amorphization observed here at 32 (10) GPa. Shock compression to pressures below the HEL (i.e., 5 GPa) permits the material to remain

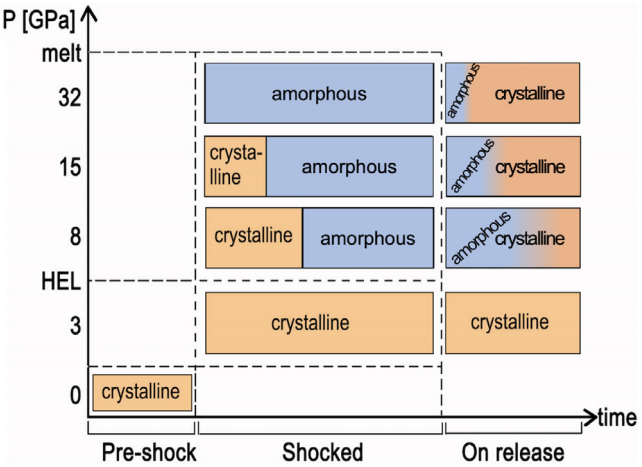

Fig. 4. Overview of the plagioclase shock process. Structural evolution of shocked, initially crystalline plagioclase. The "shocked" regime displays a qualitative representation of the relative phase fractions of crystalline and amorphous material at full compression for the indicated pressures. The "post-shock" regime indicates the morphological form of the material following release.

crystalline throughout the entirety of the shock process (Fig. 4). Above the HEL and below the melting curve, plastic flow allows the material to disorder into an amorphous phase upon compression. The structural composition of this high-pressure state varies continuously in two ways as pressure increases. First, the diffuse scattering fraction, indicative of amorphization within the shocked material, increases. Second, within the amorphous phase, a higher volume fraction forms HDA material as opposed to LDA. And on release, this material transforms to LDA. The morphological form that this quenched amorphous plagioclase occupies—nano-PDFs, micro-PDFs, or maskelynite—is dependent on the amorphous phase fraction and thus the peak pressure of the shock wave. Moreover, that morphological form is influenced by the prevalence or recovery of a crystalline matrix that is reinforced by the memory effect and the conservation of crystalline material up to 15 GPa. This is evidenced by spectroscopic studies of material from the Nördlinger Ries impact crater in Germany (e.g., Diemann & Arndt, 1984; Fritz et al., 2005; Stöffler et al., 1991; Tschermark, 1872) showing maskelynite spectral features similar to fused feldspar, despite being recovered from extreme shock conditions.

Time-resolved, ultrafast XRD was used to demonstrate the direct conversion of plagioclase to maskelynite for the first time—revealing a 5 GPa onset pressure for amorphization, which is much lower than previously suggested. The utility of high temporal fidelity XFEL probes during dynamic compression

formation uniquely reveals the nanoscale domains of amorphous plagioclase at low pressure to provide better constraints on the pressure history of plagioclase shocked to a peak pressure between 5 and 15 GPa. We find direct conversion of plagioclase to glass without the formation of a high-pressure crystalline phase transition —commonly observed under static compression. The memory effect is seen for the first time during the shock release process and from a critical pressure threshold (~30–35 GPa) where the sample converts to maskelynite or a shocked glass and then reverts to a crystalline phase, recovering its original crystallinity on a nanosecond timescale. This work demonstrates a continuous mechanism of transformation for the most common mineral in the Earth's crust and illustrates the insights that can be gained by observing the shock process with high-fidelity spatial (i.e., atomic lattice length-scales) and temporal (i.e., sub-nanosecond) resolution.

MATERIALS AND METHODS

Sample Synthesis

Polycrystalline plagioclase wafers were prepared by loading ground labradorite into 2 mm outer diameter Pt tubes, sealing the tubes by arc welding, and running eight such tubes simultaneously in an end-loaded piston cylinder press at 2.5 GPa and 1000 °C for 3 days. After 3 days at pressure and temperature, the run was cooled to 900 °C at 1 °C min^{-1} and then cooled from 900 °C to ambient temperature at 6 °C min^{-1}. The tubes were then sliced into disks with a diamond wafering saw, mounted in thermoplastic, and thinned to ~100 μm with a combination of sandpaper and diamond polishing compound. The thinned wafers were then freed by dissolving the thermoplastic in acetone and removing the Pt capsule rim, giving disks approximately 1.75 mm diameter by 0.10 mm thickness. Sample composition was measured using large-area energy-dispersive electron probe by analyzing the interiors of sintered grains. The sample composition is as follows: $Na_{0.475}Ca_{0.525}Al_{1.6}Si_{2.4}O_8$. The bulk density of our sample at ambient conditions is 2.70(3) g cc^{-1} as determined by our XRD LeBail refinement. Porosity was determined after synthesis to be on average 3%. The grain size is a few to 10 μm.

Experimental Setup

Shock experiments were performed at the matter in extreme conditions end station of the Linac Coherent Light Source, SLAC National Accelerator Laboratory. An optical laser with a 20 ns pulse duration, 250 μm spot diameter, and ~10^{12} W cm^{-2} intensity was used to shock the sample at normal incidence. The sample consisted of a 15 μm thick plastic ablator followed by 100 μm of polycrystalline labradorite.

Shock pressures were measured using VISAR, which used free surface velocities or LiF/quartz particle velocity and impedance mismatch to derive the labradorite particle velocity. However, this method does not account for possible decay of shock wave intensity as it traversed the sample. Additional VISAR data, measuring particle velocities, were collected on thinner samples to determine the pressure at intermediate positions. Extrapolation of these data to zero thickness provided a more complete pressure history of the sample. Pressures quoted throughout this paper refer to the average pressure experienced by the sample, with errors accounting for both the pressure gradient and measurement uncertainty.

The structure of the shocked material was probed using XRD with quasi-monochromatic (dE/E = 0.2–0.5%) pulsed X-rays of 50 fs pulse duration, 50 μm spot diameter, ~10^{12} photons per pulse, and 8 keV energy. The optical laser and XFEL were spatially overlapped and operated in single-shot mode. Time delay was specified for each shot, with a jitter of 0.3–0.5 ns between the optical laser and the XFEL. An oscilloscope captured each shot in order to verify the time delay. Notably, the paper defines time zero as the point at which the shock wave exits the ablator and enters the plagioclase. XRD patterns were recorded by Cornell-SLAC Pixel Array Detectors (CSPADs) which are charge integrating with 110 × 110 μm pixels operated in a single shot mode (selecting one pulse from the xFEL running at 120 Hz co-timed with the optical laser system). The XRD data were calibrated using CeO2 and LaB6 NIST powders. Analysis was completed with the Dioptas software (Prescher & Prakapenka, 2015) and masks created to eliminate the ASIC dead space between pads. A CPSAD pedestal (defined as dark current frame and bad/dead pixel map) background was applied and removed from each 2-D tiff image prior to analysis with Dioptas.

Acknowledgments—AEG and WM were supported by NSF Geophysics (EAR0738873) and AEG by Los Alamos National Laboratory (LANL) Reines LDRD and FES, DOE ECA. DRR was supported by "Materials Science of Actinides," an Energy Frontier Research Center funded by the U.S. Department of Energy (DOE) Office of Science, Basic Energy Sciences (Grant No. DE-SC0001089). This work was performed at the MEC instrument of LCLS, supported by the U.S. DOE Office of Science, Fusion Energy Science (FES) under contract No. SF00515, and was supported by

LCLS, a National User Facility operated by Stanford University on behalf of DOE-BES. Use of the LCLS, SLAC National Accelerator Laboratory, is supported by the U.S. Department of Energy, Office of Science, Office of Basic Energy Sciences under Contract No. DE-AC02-76SF00515. SHG acknowledges support by FES FWP 100182. LANL is operated for the U.S. DOE National Nuclear Security Administration under contract DE-AC52-06NA25396. This research used resources of the Advanced Light Source, which is a DOE Office of Science User Facility under contract no. DE-AC02-05CH11231. We thank LCLS/SLAC staff for assistance during/after the experiment and staff at ALS, BL 12.3.2, and insightful reviews from O. Tschauner.

Data Availability Statement—Raw data for XRD, VISAR, and drive laser profiles are all available upon reasonable request.

Editorial Handling—Dr. Natalia Artemieva

REFERENCES

Agarwal, A., Reznik, B., Kontny, A., Heissler, S., and Schilling, F. 2016. Lingunite—A High-Pressure Plagioclase Polymorph at Mineral Interfaces in Doleritic Rock of the Lockne Impact Structure (Sweden). *Scientific Reports* 6: 25991.

Ahrens, T. J., and O'Keefe, J. D. 1972. Shock Melting and Vaporization of Lunar Rocks and Minerals. *The Moon* 4: 214–49.

Ahrens, T. J., Petersen, C., and Rosenberg, J. T. 1969. Shock Compression of Feldspars. *Journal Geophysics Research* 74: 2727–46.

Barker, L. M., and Hollenbach, R. E. 1972. Laser Interferometer for Measuring High Velocities of Any Reflecting Surface. *Journal of Applied Physics* 43: 4669–75.

Becker, L., Poreda, R., Basu, A., Pope, K., Harrison, T., Nicholson, C., and Iasky, R. 2004. Bedout: A Possible End-Permian Impact Crater Offshore of Northwestern Australia. *Science* 304: 1469–76.

Benusa, M. D., Angel, R. J., and Ross, N. C. 2005. Compression of Albite, $NaAlSi_3O_8$. *American Mineralogist* 90: 1115–20.

Caracas, R., and Boffa Ballaran, R. 2010. Elasticity of (K, Na)$AlSi_3O_8$ Hollandite from Lattice Dynamics Calculations. *Physics of the Earth and Planetary Interiors* 181: 21–6.

Cygan, R. T., Casey, W., Boslough, M., Westrich, H., Carr, M., and Holden, G. Jr. 1989. Dissolution Kinetics of Experimentally Shocked Silicate Minerals. *Chemical Geology* 78: 229–44.

Dennen, R. S. 1965. *Synthesis of Rock Hugoniots*. Chicago, Illinois: DASA1652; IIT Research Institute.

Diemann, E., and Arndt, J. 1984. Diaplectic Labradorite Glass from the Manicouagan Impact Crater: II. X-Ray Diffraction Studies and Structural Model. *Physics and Chemistry of Minerals* 11: 178–81.

Emma, P., Akre, R., Arthur, J., Bionta, R., Bostedt, C., Bozek, J., Brachmann, A. et al. 2010. First Lasing and Operation of an Ångstrom-Wavelength Free-Electron Laser. *Nature Photonics* 4: 641–7.

Ferroir, T., Onozawa, T., Yagi, T., Merkel, S., Miyajima, N., Nishiyama, N., Irifune, T., and Kikegawa, T. 2006. Equation of State and Phase Transition in $KAlSi_3O_8$ Hollandite at High Pressure. *American Mineralogist* 91: 327–32.

French, B. M., and Koeberl, C. 2010. The Convincing Identification of Terrestrial Meteorite Impact Structures: What Works, What Doesn't, and Why. *Earth Science Reviews* 98: 123–70.

Fritz, J., Greshake, A., and Stöffler, D. 2005. Micro-Raman Spectroscopy of Plagioclase and Maskelynite in Martian Meteorites: Evidence of Progressive Shock Metamorphism. *Antarctic Meteorite Research* 18: 96.

Gautron, L., Angel, R., and Miletich, R. 1999. Structural Characterization of the High-Pressure Phase $CaAl_4Si_2O_{11}$. *Physics and Chemistry of Minerals* 27: 47–51.

Gibbons, R., and Ahrens, T. J. 1977. Effects of Shock Pressures on Calcic Plagioclase. *Physics and Chemistry of Minerals* 1: 95–107.

Gillet, P., Chen, M., Dubrovinsky, L., and El Goresey, A. 2000. Natural $NaAlSi_3O_8$-Hollandite in the Shocked Sixiangkou Meteorite. *Nature* 287: 1633–6.

Gleason, A. E., Bolme, C., Lee, H.-J., Nagler, B., Galtier, E., Kraus, R., Sandberg, R., Yang, W., Langenhorst, F., and Mao, W. 2017. Time-Resolved Diffraction of Shock-Released SiO_2 and Diaplectic Glass Formation. *Nature Communications* 8: 1–6.

Itie, J. P., Polian, A., Calas, G., Petiau, J., Fontaine, A., and Tolentino, H. 1989. Pressure-Induced Coordination Changes in Crystalline and Vitreous GeO2. *Physical Review Letters* 63: 398–401.

Jaret, S. J., Woerner, W. R., Philips, B. L., Ehm, L., Nekvasil, H., Wright, S. P., and Glitch, T. D. 2015. Maskelynite, Formation Via Solid-State Transformation: Evidence of Infrared and X-Ray Anisotropy. *Journal of Geophysical Research: Planets* 120: 570–87. https://doi.org/10.1002/2014JE004764.

Langenhorst, F. 1989. Experimentally Shocked Plagioclase: Changes of Refractive Indices and Optic Axial Angle in the 10–30 GPa Range. *Meteoritics* 24: 291.

Langenhorst, F. 1994. Shock Experiments on Pre-Heated α- and β-Quartz: II. X-Ray and TEM Investigations. *Earth and Planetary Science Letters* 128: 683–98.

Langenhorst, F., Joreau, P., and Doukhan, J. C. 1995. Thermal and Shock Metamorphism of the Tenham Chondrite: A TEM Examination. *Geochimica et Cosmochimica Acta* 59: 1835–45.

Langenhorst, F., and Dressler, B. 2003. First Observation of Silicate Hollandite in a Terrestrial Rock (Abstract #4046). Proceeding of the Third International Conference on Large Meteorite Impacts. Geological Society of America, Special Paper.

Liu, L. G., and El Goresey, A. 2007. High-Pressure Phase Transitions of the Feldspars, and Further Characterization of Lingunite. *International Geology Review* 49: 854–60.

Ma, C., Tschauner, O., Beckett, J., Rossman, G., Prescher, C., Prakapenka, V., Bechtel, H., and MacDowell, A. 2018. Liebermannite, $KAlSi_3O_8$, a New Shock-Metamorphic, High-Pressure Mineral from the Zagami Martian Meteorite. *Meteoritics & Planetary Science* 53: 50–61.

Meade, C., Hemley, R. J., and Mao, H. K. 1992. High-Pressure X-Ray Diffraction of SiO_2 Glass. *Physical Review Letters* 69: 1387–90.
Ostertag, R. 1983. Shock Experiments on Feldspar Crystals. *Journal of Geophysical Research* 88: 364–76.
Pittarello, L., Daly, L., Pickersgill, A., Ferriere, L., and Lee, M. 2020. Shock Metamorphism in Plagioclase and Selective Amorphization. *Meteoritics & Planetary Science* 55: 1103–15.
Posner, E., Dera, P., Downs, R., Lazarz, J., and Irmen, P. 2014. High-Pressure Single-Crystal X-Ray Diffraction Study of Jadeite and Kosmochlor. *Physics and Chemistry of Minerals* 41: 695–707.
Prescher, C., and Prakapena, V. 2015. DIOPTAS: A Program for Reduction of Two-Dimensional X-Ray Diffraction Data and Data Exploration. *High Pressure Research* 35: 223–30.
Sharp, T. G., and DeCarli, P. S. 2006. Shock Effects in Meteorites. In *Meteorites and the Early Solar System II*, edited by D. Lauretta and H. McSween Jr., 653–77. Tucson, Arizona: The University of Arizona Press.
Sims, M., Jaret, S., Carl, E.-R., Rhymer, B., Schrodt, N., Mohrholz, V., Smith, J. et al. 2019. Pressure-Induced Amorphization in Plagioclase Feldspars: A Time-Resolved Powder Diffraction Study During Rapid Compression. *Earth and Planetary Science Letters* 507: 166–74.
Sims, M., Jaret, S. J., Johnson, J. R., Whitaker, M. L., and Glotch, T. D. 2020. Unconventional High-Pressure Raman Spectroscopy Study of Kinetic and Peak Pressure Effects in Plagioclase Feldspars. *Physics and Chemistry of Minerals* 47: 12.
Stöffler, D. 1967. Deformation und Umwandlung von Plagioklas durch Stoßwellen in den Gesteinen des Nördlinger Ries. *Contributions to Mineralogy and Petrology* 16: 51–83.
Stöffler, D. 1974. Deformation and Transformation of Rock-Forming Minerals by Natural and Experimental Shock Processes: II. Physical Properties of Shocked Minerals. *Fortschritte der Mineralogie* 51: 256–89.
Stöffler, D., Keil, K., and Scott, E. 1991. Shock Metamorphism of Ordinary Chondrites. *Geochimica et Cosmochimica Acta* 55: 3845–67.
Tschauner, O. 2019. High-Pressure Minerals. *American Mineralogist* 104: 1701–31.
Tschauner, O., Luo, S. N., Asimow, P. D., and Ahrens, T. J. 2006. Recovery of Stishovite-Structure at Ambient Conditions Out of Shock-Generated Amorphous Silica. *American Mineralogist* 91: 1857–62.
Tschauner, O., Ma, C., Spray, J., Greenberg, E., and Prakapenka, V. 2021. Stofflerite, (Ca, Na)(Si, $Al)_4O_8$ in the Hollandite Structure: A New High-Pressure Polymorph of Anorthite from Martian Meteorite NWA 856. *American Mineralogist* 106: 650–5.
Tschermark, G. 1872. *Die Meteoriten von Shergotty und Gopalpur*, vol. 55, 122–145. Vienna: Sitzber. Akad. Wiss., K. K. Hof-und Staatsdruckerei.

SUPPORTING INFORMATION

Additional supporting information may be found in the online version of this article.

Fig. S1. Phase diagram of plagioclase. General phase diagram of plagioclase feldspar at equilibrium high pressure–temperature conditions. The crystalline–amorphous boundary (dashed line) is of labradorite taken from Kubo et al.[1] The green circles indicate the albite melt curve determined by Lange.[2] Extrapolation of the melt curve to higher pressures (black line) was performed by fitting the Simon–Glatzel equation. Notably, albite should provide a lower boundary to the labradorite melt temperature. Blue dashed curve is the approximate oligioclase Hugoniot.[3] For each of our peak pressures (black circles), we estimate the release path and temperatures by interpolation of post-shock temperature data reported by Ahrens et al.[3] (red dashed lines).

Fig. S2. Pressure-induced change in amorphous structure. Ratio of the intensities of the two amorphous diffraction peaks at approximately full compression (Fig. 2). I_2 corresponds to the intensity of the peak at the lower *d*-spacing, I_1 at the higher *d*-spacing. The ratio increases with pressure, which is interpreted as a decrease in medium-range order and an increase in cation coordination number within the amorphous phase. Dashed line is a guide for the eye.

Fig. S3. Two-dimensional diffraction images of shocked plagioclase. Evolution of shocked plagioclase probed at a longer time delay, during reach the laser is on release (low-pressure, high-temperature state). Integrated patterns of each image are shown beneath. During release (23–100 ns), broad and fainted rings are observed concurrent to "lens-like" features of brighter diffraction spots. This suggests that there may be a slight preferred orientation upon recrystallization during release.

Fig. S4. LeBail refinements of XRD. Full pattern refinements found using GSAS to determine the lattice parameters. Data are black crosses, calculated fits are red lines, backgrounds are green lines, the difference curves between the calculated fit and raw data are blue lines, and expected peak positions at that pressure are pink tick marks.

Fig. S5. Pressure–density comparison. A comparison of the Ahrens et al.'s[3] pressure–density data plotted with the densities determined from LeBail refinements from our XRD and using thermally corrected Benusa et al.[6] EOS to determine pressure in this work.

Fig. S6. VISAR line outs from thinner plagioclase. Uptime traces from plagioclase samples <100 μm thick + LiF to provide better fringe quality for highest pressure shots. The impedance match method was used with LiF EOS[8] and plagioclase EOS.[3]

Data S1. Supplementary text.